Title: A Gamma-adapted recombinant subunit vaccine induces broadly neutralizing antibodies against SARS-CoV-2 variants and protects mice from SARS-CoV-2 infection.

Authors:

Lorena M. Coria[a,b]*, Juan Manuel Rodriguez[c,d], Agostina Demaria[a,b], Laura A. Bruno[a,b], Mayra Rios Medrano[a,b], Celeste Pueblas Castro[a,b], Eliana F. Castro[a,b,e], Sabrina A. Del Priore[c], , Andres C. Hernando Insua[c,d], Ingrid G. Kaufmann[c], Lucas M. Saposnik[a,b], William B. Stone[f], Lineia Prado[a,b], Valeria Krum[c], Francisco M. Zurvarra[c,d], Johanna E. Sidabra[c], Ignacio Drehe[c], Jonathan A. Baqué[c], Mariana Li Causi[c], Analia V. De Nichilo[c,d], Cristian J. Payes[c], Albert J. Auguste[f,g], Julio C. Vega[h], Diego E. Álvarez[a,b], Juan M. Flo[c], Karina A. Pasquevich[a,b] and Juliana Cassataro[a,b]*.

Author Affiliations:

[a]Instituto de Investigaciones Biotecnológicas, Universidad Nacional de San Martín (UNSAM) – Consejo Nacional de Investigaciones Científicas y Técnicas (CONICET). San Martín (1650), Buenos Aires, Argentina.

[b]Escuela de Bio y Nanotecnologías (EByN), Universidad Nacional de San Martín. San Martín (1650), Buenos Aires, Argentina.

[c]Laboratorio Pablo Cassará – Unidad de I+D de Biofármacos. C1440FFX, Ciudad Autónoma de Buenos Aires, Argentina.

[d]Fundación Pablo Cassará - Unidad de I+D de Biofármacos. C1440FFX, Ciudad Autónoma de Buenos Aires, Argentina.

[e]Instituto de Virología e Innovaciones Tecnológicas (IVIT), Centro de Investigaciones en Ciencias Veterinarias y Agronómicas (CICVyA), Instituto Nacional de Tecnología Agropecuaria (INTA)- Consejo Nacional de Investigaciones Científicas y Técnicas (CONICET), Buenos Aires, Argentina.

[f]Department of Entomology, College of Agriculture and Life Sciences, Fralin Life Science Institute, Virginia Polytechnic Institute and State University, Blacksburg, VA, 24061.

[g]Center for Emerging, Zoonotic, and Arthropod-borne Pathogens, Virginia Polytechnic Institute and State University, Blacksburg, VA, 24061.

[h]Laboratorio Pablo Cassará - I+D+i. C1408GBV, Ciudad Autónoma de Buenos Aires, Argentina.

Corresponding Author: *Address correspondence to Lorena M Coria lcoria@iib.unsam.edu.ar and to Juliana Cassataro: jucassataro@iib.unsam.edu.ar

Keywords: RBD-adapted vaccine, COVID-19 subunit vaccine, SARS-CoV-2, heterologous booster.

Abstract

The COVID-19 pandemic continues with the emergence of successive new variants of concern (VOC). One strategy to prevent breakthrough infections is developing safe and effective broad-spectrum vaccines. Here, we present preclinical studies of a RBD recombinant vaccine candidate derived from the Gamma SARS-CoV-2 variant adjuvanted with alum. Gamma RBD-derived antigen elicited better neutralizing antibody and T cell responses than formulation containing ancestral RBD antigen. The Gamma-adapted subunit vaccine elicited a long-lasting antibody response with cross-neutralizing activity against different VOC including the Omicron variant. Additionally, Gamma variant RBD-adapted vaccine elicited robust T cells responses with induction of Th1 and $CD8^+$ T cell responses in spleen and lung. Vaccine-induced immunity protected K18-hACE2 mice from intranasal challenge with SARS-CoV-2 increasing survival, reducing body weight loss and viral burden in the lungs and brain. Importantly, the subunit vaccine demonstrated a potent effect as heterologous booster of different vaccine platforms including the non-replicating adenovirus vaccine ChAdOx1-S, the mRNA vaccine BNT162b2 and the inactivated SARS-CoV-2 vaccine BBIBP-CorV, increasing cross-reactive antibody responses. Our study indicates that the adjuvanted Gamma RBD vaccine is highly immunogenic and a broad-spectrum vaccine candidate to combat SARS-CoV-2 variants including Omicron.

65 **Introduction**

66 Severe Acute Respiratory Syndrome Coronavirus 2 (SARS-CoV-2) has infected
67 over 630 million people worldwide and resulted in more than 6,6 million deaths (WHO.
68 World Health Organization, Weekly Operational Update on COVID-19). The vaccines
69 authorized for emergency use or fully approved are safe and highly effective against
70 severe disease[1-5]. However, it has been reported that vaccine-induced protection
71 against symptomatic SARS-CoV-2 infection wanes over time[6,7]. Additionally, as COVID-
72 19 pandemic progresses several variants of concern (VOCs) have emerged, including
73 B.1.351 (Beta), B.1.617.2 (Delta) and P.1 (Gamma), B.1.1.529 (Omicron BA.1) and its
74 subvariants (BA.2.12.1, BA.4/BA.5, BQ.1 and XBB and its descendants). Omicron lineages
75 have been reported to be more resistant to neutralization by vaccine-elicited antibodies
76 and, in some cases are more transmissible than previous VOCs[8-12]

77 Wanning of vaccine-induced immunity and antibody evasive virus variants create
78 the need for new vaccine strategies that can induce more potent, durable, and broader
79 immune responses to enhance protection against SARS-CoV-2. Additional booster doses
80 of current vaccines have been implemented around the world. Current approved
81 vaccines are mainly directed against the spike protein of the prototype Wuhan-1 SARS-
82 CoV-2 strain therefore their efficacy against certain VOCs is limted[11]. Therefore, vaccines
83 are being adapted to variants as a strategy to improve vaccine effectiveness. While
84 current vaccines may be effective at reducing severe disease to existing VOCs, variant-
85 specific antigens, whether in a mono- or multivalent-vaccine, may be required to induce
86 optimal immune responses and reduce infection against emerging variants.

87 Most of the variant-adapted vaccines boosters were bivalent or monovalent
88 containing beta and ancestral spike antigens besides Omicron[13-16]. Interestingly, the
89 Beta variant originated in South Africa, while the Gamma variant originated in Brazil a
90 few months later. Until now, there are few studies using a Gamma variant adapted
91 vaccine [17-19].

92 In this work, we describe the design, formulation, and immunogenicity of a RBD
93 vaccine candidate comparing ancestral, and Gamma derived RBD versions. Our results
94 show that Gamma-adapted RBD vaccine is more immunogenic than ancestral RBD
95 vaccine in terms of inducing broader neutralizing antibodies (and higher antigen (Ag)
96 specific cellular immune responses. Therefore, we selected RBD Gamma as antigen to
97 develop a recombinant subunit vaccine that can be used as primary or booster vaccine.
98 Here we describe the rational design, generation, and preclinical evaluation of the
99 Gamma RBD-based vaccine candidate using aluminum hydroxide as adjuvant.
100 Immunogenicity was evaluated after a primary two-dose vaccine schedule and after a
101 heterologous booster of different anti-SARS-CoV-2 vaccine platforms including the non-
102 replicating adenovirus vaccine ChAdOx1-S (Oxford AstraZeneca), the mRNA vaccine
103 BNT162b2 (Pfizer) and the inactivated SARS-CoV-2 vaccine BBIBP-CorV (Sinopharm).

104 **Results**

105 ***Design and production of RBD antigens***

106 To compare immune responses elicited with ancestral or Gamma derived RBD,
107 two formulations were developed using RBD homodimers from the ancestral (Wuhan-
108 Hu-1) and Gamma variants. Antigens comprise single-chain dimeric repeats of the RBD
109 protein from amino acids 319R to 537K. The Gamma RBD antigen includes the mutations

110 described in the Gamma SARS-CoV-2 variant of spike in this region: K417T; E484K and
111 N501Y (P.1/501Y.V3). High-productivity clones were generated under the genetic
112 background of a CHO-S (Chinese Hamster Ovary) cell line in high-density suspension cell
113 cultures. Then, proteins were purified, and antigen purity confirmed by SDS-PAGE and
114 Western Blot (**Fig. 1A-B**). Comparison of the binding affinity of Gamma and ancestral
115 RBD to hACE2 receptor was performed by ligand-receptor binding ELISA (**Fig. 1C**). Both
116 antigens bind to hACE2 at comparable levels with a slight greater binding affinity of
117 Gamma RBD. Purified antigens were then absorbed to aluminum hydroxide (alum) to
118 generate the final formulations.

119 ***Gamma RBD antigen vaccine formulation improved antibody and cellular immune***
120 ***responses in comparison with ancestral RBD antigen.***

121 Immunogenicity of vaccine formulations was assessed in BALB/c mice after i.m.
122 immunization in a two-dose vaccine schedule using 10µg of each antigen absorbed in
123 aluminum hydroxide (**Fig. 2A**). RBD (Gamma and ancestral)-specific IgG was evaluated
124 by ELISA in sera of immunized animals. Both formulations induced high levels of IgG
125 antibodies against the ancestral and Gamma RBD antigens (**Fig. 2B**). Anti-RBD IgG
126 responses elicited by the formulation containing the Gamma antigen were significatively
127 higher than that induced by the ancestral RBD-based vaccine on days 14 and 42 after
128 prime immunization (**Fig. 2C**).

129 Neutralizing antibody activity was evaluated by a live virus assay using ancestral
130 or Gamma SARS-CoV-2 variants. Immunization with the formulation containing
131 ancestral RBD antigen induced higher neutralization titers against ancestral SARS-CoV-2
132 than against Gamma variant (**Fig. 2D**, $p<0.05$ NT50 Gamma vs ancestral, time points
133 from 14 to 35 days post prime immunization). In contrast, vaccination with Gamma RBD

134 plus Alum elicited high neutralizing antibody (Ab) titers against both viruses. In addition,
135 cellular immune responses were analyzed in splenocytes from immunized animals by
136 intracellular flow cytometry. Gamma RBD-based vaccine induced higher frequency of
137 IFN-γ and TNF-α producing $CD4^+$ and $CD8^+$ T cells ($p<0.05$, medium alone vs RBD peptides
138 stimulation) compared to the frequency induced by the formulation with the ancestral
139 RBD antigen (**Fig. 2E**). These results demonstrated that vaccine containing Gamma RBD
140 antigen induces a broader neutralizing response and a superior Ag-specific T cellular
141 immune response than RBD derived from the ancestral SARS-CoV-2. Thus, we decided
142 to move forward with the formulation containing the Gamma RBD antigen.

143 ***Gamma RBD adjuvanted formulation induces long-lasting antibody responses with***
144 ***broad neutralizing activity against different virus variants of concern***

145 Binding antibody responses were evaluated over longer periods after mice
146 immunization revealing that anti-RBD IgG titers remained high up to 253 days (more
147 than 8 months) post prime immunization (**Fig. 3B**). Additionally, neutralization capacity
148 of antibodies elicited after immunization was evaluated using different VOCs in a live
149 virus PRNT assay at this time point. Immunization with Gamma RBD adsorbed to Alum
150 elicited high neutralizing Ab titers against Gamma (GMT 254.8) and ancestral (GMT
151 312.8) virus. Interestingly, elicited antibodies showed cross-reactivity against Alpha
152 (GMT 67.82), Delta (GMT 85.49), Omicron BA.1 (GMT 135.5) and BA.5 (GMT 33.12) VOCs
153 (**Fig. 3B**). Of note, there were no significant differences between these variants
154 indicating that Gamma RBD vaccination elicits broadly long-lasting neutralizing Ab
155 responses.

156

157 ***Gamma RBD-adapted vaccine elicits Ag-specific mixed Th1-Th2 immune responses***

158 Figure 2 shows that Gamma RBD adjuvanted formulation induces Ag-specific T
159 cell responses in splenocytes. The cell-mediated immune responses in spleen and lung
160 generated after vaccination was further evaluated. Gamma RBD plus alum vaccination
161 induced Ag-specific IFN-y and IL-5 secretion in spleen and lung cells (**Fig. 4A**) indicating
162 that a mixed Th1/Th2 is generated at local and systemic level.

163 In the spleen, antigen-specific IFN-y- and TNF-α-producing $CD4^+$ T cells and IFN-y
164 producing $CD8^+$ T cells were detected upon Ag stimulation of cells from vaccine
165 immunized group (**Fig. 4B**). In the lung, immunization with Gamma RBD + Alum elicited
166 RBD-specific IFN-y producing $CD4^+$ T cells (**Fig. 4C**). Production of cytokines by $CD8^+$ T
167 cells was not detected in the lungs (data not shown).

168 A large proportion of antigen-specific cytokine producing $CD4^+$ T and $CD8^+$ T cells
169 in spleens were double positive IFN-y^+ TNF- α^+ and single positive IFN-y^+ Th1 cells (**Fig.**
170 **4D-E**). Analysis of total $CD4^+$ and $CD8^+$ T cell population that produce cytokines revealed
171 that induced multifunctionality is greater in the population of $CD8^+$ T cells (**Fig. 4E**).

172 These results suggest that the Gamma RBD-based vaccine promotes a specific T
173 cell response biased to a multifunctional Th1 profile and effector $CD8^+$ T cells able to
174 produce IFN-y in spleen. Interestingly, a Th1 response with production of IFN-y was
175 observed in the lungs.

176 ***Gamma RBD-based vaccine protects mice after intranasal SARS-CoV-2 challenge***

177 To determine vaccine ability to protect against SARS-CoV-2 infection, a lethal K-
178 18-hACE2 transgenic mice model was used[20,21]. Immunized mice were challenged
179 intranasally with $2x10^5$ PFU of SARS-CoV-2 and monitored daily for body weight changes

180 and survival, a subset of mice was euthanized on day 5 post-infection (p.i.) to measure
181 viral loads in the lungs and brains.

182 Body weight started to decrease in infected placebo mice after 3 days p.i.
183 reaching a 20% body weight decrease on day 9 p.i. whereas mice immunized with the
184 vaccine did not show significant weight loss during the experiment (**Fig. 5A**). Moreover,
185 80% of infected placebo mice died approximately 6 days p.i., 83% of vaccine immunized
186 mice where alive at this time point. (**Fig. 5B**). After 9 days, all mice in the placebo group
187 succumb to infection whereas a 66% of the immunized mice survived (P = 0.0208
188 vaccinated vs placebo).

189 Five days post infection, a subset of animals was euthanized to assess viral loads
190 in the lungs and brains. High infectious SARS-CoV-2 titers were observed in the lungs
191 and brains of the placebo group of mice while low virus titers were detected in brains of
192 animals vaccinated with Gamma RBD + Alum (**Fig. 5C**). Thus, the Gamma RBD-based
193 vaccine induced protection against experimental intranasal challenge with SARS-CoV-2
194 in a mouse model of severe disease.

195 ***A booster dose of Gamma RBD-based vaccine induces higher neutralizing Ab titers***
196 ***than homologous booster vaccination in mice previously primed with different vaccine***
197 ***platforms.***

198 Booster vaccination has become a strategy to prevent SARS-CoV-2 breakthrough
199 infections. Immunogenicity of the Gamma RBD adjuvanted vaccine as a heterologous
200 booster for different primary vaccine platforms was studied in comparison with
201 homologous regimens (i.e., three dose of the same vaccine). To this end, each group of
202 mice was immunized with one of the following vaccine platforms in a two-dose scheme

203 primary vaccination: i) non-replicating adenovirus vaccine ChAdOx1-S (Oxford
204 AstraZeneca), ii) the mRNA vaccines BNT162b2 (Pfizer) and iii) the inactivated SARS-CoV-
205 2 vaccine BBIBP-CorV (Sinopharm). Three months later, half of the animals received a
206 homologous boost and the other half a heterologous boost with the Gamma RBD-based
207 vaccine (**Fig. 6A**).

208 All vaccine platforms induced RBD-specific IgG after two dose primary
209 vaccination (**Fig 6B**). Interestingly, three months after primary vaccination the Gamma
210 RBD-based vaccine candidate elicited the highest Ab titers (day 98 post prime
211 immunization, **Fig. 6B**). Three weeks after the third dose, in the group that received a
212 primary regimen with the inactivated BBIBP-CorV- vaccine the increase in RBD-specific
213 IgG titers was higher after homologous boosting with Gamma-adapted vaccine than
214 with the homologous vaccine (18.4× vs. 4×-fold-increase respectively, $p<0.05$). Similarly,
215 primary vaccination with the non-replicating adenovirus vaccine group ChAdOx1-S and
216 booster with Gamma RBD vaccination showed a higher fold-increase in anti-RBD IgG
217 titers than homologous ChAdOx1-S boosting (13.9× vs. 0.65×-fold-increase respectively,
218 $p<0.001$. **Fig. 6C**). In the group that received mRNA vaccine as primary regimen the
219 increment in RBD-specific IgG titers was similar after homologous or heterologous
220 booster (6× vs. 4× fold rise respectively, $p>0.05$. **Fig. 6C**).

221 Analysis of the neutralizing activity of sera from mice before (pre) and after
222 booster (post) immunization against ancestral SARS-CoV-2 revealed that the fold-
223 increase in neutralizing Ab titer were significantly higher after heterologous booster
224 with the Gamma subunit vaccine than homologous booster with BBIBP-CorV and
225 ChAdOx1-S vaccines (**Fig. 6D,** $p<0.05$). Heterologous boosting with the Gamma subunit

226 vaccine induced a significantly higher increase of the neutralizing Abs titers against the
227 Gamma VOC than homologous boosting in all vaccine platforms used to prime mice (**Fig.**
228 **6D**). The best neutralization activity (against ancestral and Gamma variants) was
229 observed in the group that received primary immunization with the mRNA vaccine
230 BNT162b2 and boosted with the Gamma RBD-adapted vaccine (**Fig 6D**).

231 Finally, cross-neutralization activity was assessed against Omicron subvariants
232 BA.1 and BA.5 three weeks after the booster dose. In all groups, antibody neutralization
233 capacity was reduced against Omicron subvariants compared to neutralizing Ab titers
234 against the ancestral and Gamma variant. However, a degree of cross-reactive
235 antibodies against BA.1 and BA.5 was detected, and the groups boosted with the subunit
236 vaccine outperformed groups boosted with homologous vaccines (adenoviral,
237 inactivated and mRNA vaccines, **Fig. 6 D-E**). In particular, in the group that received
238 mRNA as primary vaccination, the neutralizing Ab titers against Omicron BA.1 and BA.5
239 were significantly higher after a heterologous boost with Gamma RBD-adapted subunit
240 vaccine than with a homologous boost vaccination **(Fig. 6D-E)**.

241 These results suggest that the Gamma RBD-adapted recombinant vaccine
242 candidate could serve as an effective booster of different primary vaccine platforms
243 inducing a broad cross-reactive immunity.

244 **Discussion**

245 The rapid emergence of SARS-CoV-2 variants has challenged the global
246 development of vaccines. The ability of VOCs to escape neutralization by antibodies
247 elicited by infection, vaccination, or therapeutic application has been widely
248 studied[22,23]. Developing variant adapted vaccines that can elicit broad and strong

249 immune responses against these predominant circulating variant(s) is proposed as one
250 of the best strategies to address variants immune evasion.

251 In this study, we described the immunogenicity of a recombinant adapted
252 subunit vaccine formulated with aluminum hydroxide to be used as a primary or booster
253 vaccine. Ancestral and Gamma variant derived RBD antigens were compared in their
254 capacity to induce neutralizing Ab responses against SARS-CoV-2. It was reported that
255 sera from individuals vaccinated with an ancestral RBD antigen plus alum vaccine
256 formulation showed a reduction in neutralizing antibody titers of 1.7x and 2.1x fold
257 against Gamma and Beta variants of SARS-CoV-2 respectively[24]. In agreement with these
258 results ancestral RBD could not induce good neutralizing activity against the Gamma
259 SARS-CoV-2 variant whereas we demonstrated for the first time that the vaccine
260 formulation containing Gamma RBD was able to induce neutralizing Abs against
261 ancestral and Gamma SARS-CoV-2 variants.

262 Beta and Gamma variants, which originated in South Africa and Brazil,
263 respectively, carry the K417N/T, E484K and N501Y amino acid changes in the spike RBD.
264 Mutations in the Beta variant decreased the neutralization sensitivity of convalescent
265 and vaccinated sera by 6x-fold, while mutations in Gamma decreased neutralizing
266 activity by 3x-fold [25]. Mono and bivalent candidates containing different combinations
267 of VOCs based antigens have been assessed in humans [13,26]. Omicron-adapted mRNA
268 vaccines as boosters have been implemented in several countries. Recently, a Beta-
269 adapted subunit vaccine has been approved for use in Europe. Until present, there are
270 no clinical studies with a Gamma adapted vaccine.

271 The Gamma variant booster vaccine candidate tested here showed a broad cross-
272 reactive neutralizing antibody response against several VOCs including Omicron in mice.
273 This could be related to the notion that K417N/T and E484K substitutions shared by Beta
274 and Gamma viruses simulate a structure that enhances the spectrum of neutralizing
275 activity. In agreement with this hypothesis and our results, a study evaluating the
276 immunogenicity of an S-protein sequence containing these three substitutions in
277 addition to D614G (B.1) demonstrated that the variant vaccine is capable of eliciting high
278 neutralizing Ab titers that cross-reacted with five VOCs in NHP[27]. Moreover, in preclinical
279 and clinical trials Beta derived vaccines induced broadly neutralizing antibodies that can
280 cross-react against different VOC [27,28] in a similar way than the Gamma derived vaccine
281 presented in this work.

282 A recombinant vaccine containing RBD-dimers derived from ancestral SARS-CoV-
283 2 and aluminum hydroxide as adjuvant proved to be safe and immunogenic in humans[29].
284 Structural analysis of these RBD-dimers indicates that are arranged in a way where the
285 receptor binding motif (RBM) is correctly presented and the major antigenic sites of RBD
286 are exposed[30]. This supports the versatility of the RBD-dimers as a module to adapt
287 different variants for the induction of broader immune responses. Hence, it has been
288 reported that chimeric RBD-dimers elicit broader responses to variants compared with
289 homodimers[30]. Increasing evidence suggests that vaccine protection against COVID-19
290 might be waning over time, and newly emerging variants, such as Delta and Omicron,
291 might evade vaccine-induced immune protection. Our vaccine induced a long-lasting
292 antibody response with neutralizing activity against different VOCs up to 253 days after
293 the last immunization. Adjuvanted recombinant COVID-19 vaccine formulations have
294 reported durability of the neutralizing-antibody responses for 7 months post-

295 immunization in NHP[31]. This study together with previous reports suggest that
296 recombinant variant-specific vaccines may be needed for improved and long-lasting
297 protection against known and emerging VOCs.

298 Main correlates of protection against COVID-19 are binding and neutralizing
299 antibody titers[32]. However, cellular immunity is associated with positive outcomes[33].
300 Here, we have provided a comprehensive assessment of the T cell response to a Gamma-
301 adapted recombinant subunit vaccine. Gamma RBD + alum vaccination elicited a robust
302 Th1-dominated T cell response and RBD-specific $CD8^+$ T cell response. Analysis of
303 polyfunctionality on vaccine elicited T cells suggests that the major proportion of cells
304 produce one or two cytokines (IFN-γ and TNF-α). Polyfunctional Th1 responses were
305 reported after human vaccination with adenoviral ChAdOx1-S and the mRNA BNT162b2
306 vaccine[34,35]. Protection studies in transgenic mice presented here confirm that the
307 immunity induce by the Gamma-derived RBD vaccine candidate can protect mice from
308 a lethal nasal challenge of ancestral SARS-CoV-2 virus.

309 Updated immunization strategies were implemented as booster shots across the
310 globe. In this work, we showed that vaccination with Gamma RBD plus alum as booster
311 of adenoviral, inactivated or mRNA-based vaccines induced a higher binding and
312 neutralizing antibody titer increase against different VOCs than vaccinations with
313 homologous vaccines. In general, heterologous boosters showed higher vaccine
314 effectiveness than homologous boosters for all outcomes in humans, providing
315 additional support for a mix-and-match approach[36,37]. Our vaccine not only increased
316 GMT values of neutralizing Ab against ancestral and Gamma virus variants but also
317 against Omicron lineages (BA.1 and BA.5).

318 The Gamma-RBD vaccine candidate reported in this article has demonstrated to
319 be safe in non-clinical safety studies. Both the antigen and the formulated vaccine are
320 being produced under GMP at manufacturing plants of Laboratorio Pablo Cassará S.R.L.
321 located in Buenos Aires. Stability studies showed that the vaccine can be stored and
322 handled in refrigerated conditions (2 – 8 °C) and does not need freezing temperatures.
323 The development of a vaccine does not require stringent cold-chain transport and
324 storage facilitates its availability at local and global supply. This gamma RBD plus alum
325 vaccine was named ARVAC Cecilia Grierson and is currently in a Phase 1 clinical trial
326 (NCT05656508).

327 This work highlighted the value of a Gamma variant-adapted vaccine to induce
328 higher and broader immune responses against SARS-CoV-2 at booster vaccination and
329 set the precedent for its further clinical development.

330 **Methods**

331 **Antigen expression and purification**

332 Constructs from Wuhan (ancestral) and Gamma SARS-CoV-2 variants of the antigen
333 consisted of a single-chain dimer of the receptor binding domain (RBD), comprising
334 amino acids 319R to 537K of the Spike protein from ancestral and Gamma virus variant.
335 The signal peptide sequence from the SARS-CoV-2 Spike protein was used for protein
336 secretion. The constructs were codon-optimized for CHO cell expression and
337 synthesized by GenScript (Hong Kong Limited, Japan). All constructs were cloned into
338 the pJC3UMCS-4 expression vector (Pablo Cassara Foundation) comprising a CMV
339 promoter and a cis-acting sequence for minimized host gene silencing. Linearized forms
340 of the vectors were transfected into CHO-S cells by lipofection. After 15-20 days of G418
341 antibiotic selection, an end point dilution procedure was applied for clone isolation.

342 Clone candidates were selected by specific and volumetric productivity assessed by
343 ELISA. Recombinant protein relative abundance was confirmed by SDS-PAGE and
344 Coomasie Brilliant Blue G-250 staining.

345 Pilot batches of antigen and vaccines were manufactured by Laboratorio Pablo Cassará,
346 Argentina. Controlled cell substrates were used to inoculate a 2-L bioreactor with 1.4 L
347 as working volume. An alternate tangential flow system (ATF, Repligen) was used for
348 perfusion. The harvest after 20 - 25 days was used as starting material for a downstream
349 process based on three chromatographic steps: first an affinity mix-mode capture
350 chromatography step followed by two different ionic chromatography to eliminate
351 residual host cell DNA and host cell proteins and other process-related impurities. TFF
352 (Tangential flow filtration) was used to adjust pH, conductivity, and protein
353 concentrations of the batches.

354 **SDS-PAGE and western blot analysis**

355 RBD samples were run under reducing and non-reducing conditions by SDS-PAGE (10%
356 polyacrylamide). The samples were visualized by staining with Coomassie Brilliant Blue
357 G-250. Bands were then transferred to a nitrocellulose membrane (Bio-Rad Inc.
358 Hercules, CA, USA), blocked with Non-fat milk 5% in phosphate buffered saline (PBS)-
359 Tween 0.05%, and incubated with anti-RBD rabbit polyclonal serum (1/1000 dilution).
360 An anti-rabbit IgG horseradish-peroxidase conjugated (1/2000 dilution) was used as a
361 secondary antibody (Agilent DAKO, Santa Clara, CA, USA) and 4-Chloro-1-Naphthol as
362 substrate for colorimetric detection.

363 **ACE2 binding to RBD analyzed by titration ELISA**

364 ACE2 binding to the produced RBD variant antigens was analyzed by ELISA. Briefly, 0.1ug
365 of RBD per well was immobilized on a High binding Microplatte (Greiner Bio-One GmbH,
366 Austria.) and incubated ON at 4°C. Next, plates were blocked with 5% non-fat milk in
367 PBS 0.05% Tween20 for 2 h at 37°C and then washed with PBS and 0.05% Tween20.
368 Plates were then incubated with hACE2 (R&D, Minneapolis MN, USA) for 2 h at 37°C and
369 another washing step was performed. Finally, plates were incubated with anti-hACE2
370 (R&D Systems) diluted in 1% non-fat milk PBS 0.05% Tween 20 for 2 h at 37°C. Detection
371 was performed with a secondary Ab conjugated to HRP (Agilent DAKO, Santa Clara, CA,
372 USA) and visualized with tetramethylbenzidine (TMB) substrate (BD biosciences,
373 Franklin Lakes, New Jersey, USA).

374 **Adjuvant and formulations**

375 Pilot batches of vaccines were manufactured using aluminum hydroxide as adjuvant.
376 The antigen was adsorbed onto the adjuvant by mixing. Free antigen was controlled to
377 be less than 10% of total antigen in the vaccine.

378 **Ethics statement**

379 All experimental protocols with animals were conducted in strict accordance with
380 international ethical standards for animal experimentation (Helsinki Declaration and its
381 amendments, Amsterdam Protocol of welfare and animal protection and National
382 Institutes of Health, NIH USA, guidelines.). The protocols performed were also approved
383 by the Institutional Committee for the use and care of experimental animals (CICUAE)
384 from National University of San Martin (UNSAM) (01/2020).

385 **Animals and immunizations**

386 Eight-week-old female BALB/c mice were obtained from IIB-UNSAM animal facility.
387 Animals were intramuscularly (i.m) inoculated at day 0 and 14 with i) Gamma RBD (10µg)
388 + Alum (n=5), ii) ancestral RBD (10µg) + Alum (n=5), iii) placebo (n=4). In other
389 experiments, i) Gamma RBD (10µg) + Alum (n=5) and ii) placebo (n=5). Blood samples
390 were collected weekly to measure total and neutralizing antibody titers and at day 42
391 post prime immunization animals were sacrificed and spleens and lungs harvested.

392 **Determination of antibody levels in serum**

393 RBD-specific antibody responses (IgG) were evaluated by indirect ELISA as described
394 previously[38]. Briefly, plates were coated with 0.1 µg/well of RBD (derived from ancestral
395 or Gamma variant) in phosphate buffered saline (PBS) overnight at 4 °C. Plates were
396 washed and then incubated with diluted sera and then plates were washed and
397 incubated with HRP conjugated anti-mouse IgG (SIGMA, St. Louis, MO, USA). Results
398 were read at 450 nm to collect end point ELISA data. End-point cut-off values for serum
399 titer determination were calculated as the mean specific optical density (OD) plus 3
400 standard deviations (SD) from sera of saline immunized mice and titers were established
401 as the reciprocal of the last dilution yielding an OD higher than the cut-off.

402 **Viruses**

403 Ancestral SARS-CoV-2 (B.1, GISAID Accession ID EPI_ISL_16290469), Alpha (B.1.1.7
404 GISAID Accession ID EPI_ISL_15806335), Gamma (P.1, GISAID Accession ID
405 EPI_ISL_15807444) and Omicron BA.5 (GISAID Accession ID EPI_ISL_16297058) were
406 isolated from nasopharyngeal specimens at the Instituto de Investigaciones
407 Biotecnológicas (IIB, UNSAM) and adapted in Vero E6 cultures. Delta SARS-CoV-2
408 (GISAID Accession ID: EPI_ISL_11014871) and Omicron BA.1 (GISAID Accession ID

409 EPI_ISL_10633761) were isolated at Instituto de Investigaciones Biomédicas en
410 Retrovirus y SIDA (INBIRS, UBA-CONICET) from nasopharyngeal swabs of patients.
411 Studies using SARS-CoV-2 were done in a Biosafety level 3 laboratory at IIB, UNSAM, and
412 the protocol was approved by the INBIRS Institutional Biosafety Committee.

413 **SARS-CoV-2 neutralization assay**

414 Serum samples were heat-inactivated at 56°C for 30 min. Serial dilutions were
415 performed and then incubated for 1 h at 37ºC in the presence of 300 $TCID_{50}$ of SARS-
416 CoV-2 in DMEM 2% FBS. One hundred µl of the mixtures were then added onto Vero
417 cells monolayers. After 72 h at 37ºC and 5% CO_2, cells were fixed with PFA 4% (4°C
418 overnight) and stained with crystal violet solution in methanol. The cytopathic effect
419 (CPE) of the virus on the cell monolayer was assessed by surface scanning at 585 nm in
420 a microplate reader (FilterMAx F5 Microplate reader, Molecular Devices, San Jose, CA,
421 USA). Average optical density (OD) of each well was used for the calculation of the
422 percentage of neutralization of viral CPE for each sample as: Neutralization% = 100 x (DO
423 $_{sample}$ - DO $_{virus\ control}$) / (DO $_{cell\ control}$ - DO $_{virus\ control}$). Non-linear curves of Neutralization
424 (%) vs. Log 1/sera dilution were fitted to obtain the titer corresponding to the 50% of
425 neutralization (NT50).

426 **Determination of T cell immune responses**

427 Four weeks after the second dose, mice were sacrificed to study cellular responses.
428 Splenocytes were cultured for 5 days in the presence of RBD antigen (ancestral or
429 Gamma) or complete medium. Then, supernatants were collected, and cytokines (IFN-y
430 and IL-5) were measured by ELISA (Biolegend. San Diego, CA). For intracellular cytokine
431 determination: splenocytes were cultured ($4x10^6$ cells/well) in the presence of stimulus

432 medium (complete medium supplemented with anti-CD28 and anti-CD49d) or Ag stimuli
433 (stimulus medium + RBD-peptides + RBD protein) for 18 h. Next, brefeldin A was added
434 for 5 h to the samples. Cells were then washed, fixed, permeabilized, stained, and
435 analyzed by flow cytometry. The cells were stained with Viability dye (Zombie Acqua),
436 anti-mouse-CD8a Alexa Fluor 488, anti-mouse-CD4 Alexa Fluor 647, anti-IL-4 Brilliant
437 Violet 421, anti-TNFα PeCy7 and anti-IFN-γ PE (Biolegend. San Diego, CA). BD Fortessa
438 LSR-X Cytometer with DIVA Software were used for analysis.

439 **SARS-CoV-2 challenge of vaccinated K18-hACE2 mice**

440 Four-week-old K18-hACE2 mice from Jackson Laboratory were used for evaluating
441 vaccine efficacy. Mice were separated into two groups: i) control (n=8) Placebo (PBS)
442 and Gamma RBD +Alum (n=9). Mice in each group included males and females. They
443 were i.m immunized on day 0 and 14 as described for immunogenicity assays. Four
444 weeks post second vaccination, mice were challenged intranasally (i.n.) with 10^5 PFU of
445 SARS-CoV-2 strain WA1/2010 split evenly in each nare. Mice were monitored daily for
446 weight loss and signs of disease for two weeks post-challenge. Three mice per group
447 were euthanized on day 5 post-challenge to evaluate organ viral loads, by plaque assay
448 on Vero E6 cells as previously described[38].

449 **Statistical analysis**

450 Statistical analysis and plotting were performed using GraphPad Prism 8 software
451 (GraphPad Software, San Diego, CA). In experiments with more than two groups, data
452 were analyzed using one-way ANOVA with Kruskal Wallis or Bonferroni post-test. When
453 necessary, a logarithmic transformation was applied prior to the analysis to obtain data
454 with a normal distribution. In experiments with two groups, an unpaired t test or Mann–

455 Whitney U test were used. A p value <0.05 was considered significant. When bars were
456 plotted, results were expressed as means ± SEM for each group. Survival curves were
457 analyzed using Long-rank test.

458 **Data availability**

459 The authors declare that the data supporting the findings of this study are available from
460 the corresponding author upon reasonable request.

461 **Acknowledgements**

462 The authors are grateful to the technical staff at the I+D Biofármacos Laboratorio Pablo
463 Cassará and to Fundación Pablo Cassará for their significant assistance in the
464 preparation and control of the antigen pilot lots and the regulatory documentation:
465 Cintia Parsza, Brenda Heinrich, Melisa Gambone, Horacio Descoins, Christian Cortez,
466 María Victoria Román and Romina Albarracín. The authors would also like to thank
467 Danielle Porier, Krisangel López, and Manette Tanelus for technical assistance with the
468 SARS-CoV-2 challenge studies. We thank Ministerio de Salud de la Provincia de Buenos
469 Aires for providing mRNA, adenoviral and inactivated vaccines.

470 **Contributions**

471 L.M.C. was responsible of overall experiment design, conducted humoral and cellular
472 experiments, collected data, performed data analysis, and wrote the manuscript. J.C.
473 was responsible for overall experimental design and conceptualization, wrote the
474 manuscript and received funding support. J.M.R. generated high expression vectors,
475 designed the antigen and was responsible of development of the vaccine formulation
476 and downstream development. Coordination of antigen and vaccine production. K.A.P.
477 and J.M.F. participated of experimental design, data analysis and reviewed the

manuscript. D.E.A. designed and supervised neutralization studies and analysis. A.D. conducted and analyzed humoral studies and conducted cellular studies. C.P.C., L.A.B, L.M.S and L.P. conducted humoral and cellular studies. M.R.M. and E.F.C. performed virus neutralization studies and data analysis. S.A.DP. generated high expression vector and optimization of high productive clones. A.C.HI. Responsible of upstream and downstream development of antigens. I.G.K. coordinated overall analytics procedures, developed validation and analytics methodologies, performed structural characterization of antigen and vaccine formulation. A.V.DN. generated cell banks, performed stability, clones purity and identity studies. V.K. and I.D. generated, characterized, and screened cell clones. F.M.Z., J.A.B. and C.J.P performed upstream and downstream development of antigen. J.E.S. and M.LC. participated in the development of validation and analytics methodologies, performed structural characterization of antigen and vaccine formulation and performed animals studies. J.C.V. participated in the development of vaccine formulation, collaborates in the overall process of vaccine development. A.J.A. design, supervise and conduct animal challenge studies and data analysis. W.B.S. performed animal challenge studies and data analysis. All authors revised the manuscript.

Competing interest

J.M.R., A.C.HI., F.M.Z. are salaried employees of Fundacion Pablo Cassara. S.A.DP., I.G.K., A.V.DN., V.K., I.D., C.J.P., J.A.B., J.E.S., M.LC., J.M.F. and J.C.V. are salaried employees of Laboratorio Pablo Cassara. L.M.C., J.C., K.A.P., D.E.A., A.D., C.P.C., L.A.B, L.M.S., L.P., M.R.M., E.F.C. A.J.A. and W.B.S. declare no competing interests relevant to this article.

Funding

This work was supported by Laboratorio Pablo Cassará and grants from Agencia Nacional de Promoción de la Investigación, el Desarrollo Tecnológico y la Innovación (AGENCIA I+D+i) and Ministerio de Ciencia, Tecnología e Innovación (FONARSEC 0001) to J.C. and from the National Institute of Allergy and Infectious Diseases of the National Institutes of Health under Award Number R01AI153433 to A.J.A.

References

1 Baden, L. R. *et al.* Efficacy and Safety of the mRNA-1273 SARS-CoV-2 Vaccine. *New England Journal of Medicine* **384**, 403-416, doi:10.1056/nejmoa2035389 (2021).

2 Bos, R. *et al.* Ad26 vector-based COVID-19 vaccine encoding a prefusion-stabilized SARS-CoV-2 Spike immunogen induces potent humoral and cellular immune responses. *npj Vaccines* **5**, doi:10.1038/s41541-020-00243-x (2020).

3 Polack, F. P. *et al.* Safety and Efficacy of the BNT162b2 mRNA Covid-19 Vaccine. *New England Journal of Medicine* **383**, 2603-2615, doi:10.1056/nejmoa2034577 (2020).

4 Voysey, M. *et al.* Safety and efficacy of the ChAdOx1 nCoV-19 vaccine (AZD1222) against SARS-CoV-2: an interim analysis of four randomised controlled trials in Brazil, South Africa, and the UK. *The Lancet* **397**, 99-111, doi:10.1016/s0140-6736(20)32661-1 (2021).

5 Al Kaabi, N. *et al.* Effect of 2 Inactivated SARS-CoV-2 Vaccines on Symptomatic COVID-19 Infection in Adults. *JAMA* **326**, 35, doi:10.1001/jama.2021.8565 (2021).

524 6 Chemaitelly, H. *et al.* Waning of BNT162b2 Vaccine Protection against SARS-CoV-
525 2 Infection in Qatar. *New England Journal of Medicine* **385**, e83,
526 doi:10.1056/nejmoa2114114 (2021).
527 7 Goldberg, Y. *et al.* Waning Immunity after the BNT162b2 Vaccine in Israel. *New*
528 *England Journal of Medicine* **385**, e85, doi:10.1056/nejmoa2114228 (2021).
529 8 Wang, Q. *et al.* Antibody evasion by SARS-CoV-2 Omicron subvariants BA.2.12.1,
530 BA.4 and BA.5. *Nature* **608**, 603-608, doi:10.1038/s41586-022-05053-w (2022).
531 9 Khan, K. *et al.* Omicron BA.4/BA.5 escape neutralizing immunity elicited by BA.1
532 infection. *Nature Communications* **13**, doi:10.1038/s41467-022-32396-9 (2022).
533 10 Tuekprakhon, A. *et al.* Antibody escape of SARS-CoV-2 Omicron BA.4 and BA.5
534 from vaccine and BA.1 serum. *Cell* **185**, 2422-2433.e2413,
535 doi:10.1016/j.cell.2022.06.005 (2022).
536 11 Tseng, H. F. *et al.* Effectiveness of mRNA-1273 against SARS-CoV-2 Omicron and
537 Delta variants. *Nature Medicine* **28**, 1063-1071, doi:10.1038/s41591-022-01753-
538 y (2022).
539 12 Suryawanshi, R. K. *et al.* Limited cross-variant immunity from SARS-CoV-2
540 Omicron without vaccination. *Nature* **607**, 351-355, doi:10.1038/s41586-022-
541 04865-0 (2022).
542 13 Chalkias, S. *et al.* A Bivalent Omicron-Containing Booster Vaccine against Covid-
543 19. *New England Journal of Medicine* **387**, 1279-1291,
544 doi:10.1056/nejmoa2208343 (2022).
545 14 Akache, B. *et al.* Immunogenicity of SARS-CoV-2 spike antigens derived from Beta
546 & Delta variants of concern. *npj Vaccines* **7**, doi:10.1038/s41541-022-
547 00540-7 (2022).

548 15 Sridhar, S. *et al.* The potential of Beta variant containing COVID booster vaccines
549 for chasing Omicron in 2022. *Nature Communications* **13**, doi:10.1038/s41467-
550 022-33549-6 (2022).
551 16 Launay, O. *et al.* Immunogenicity and Safety of Beta-Adjuvanted Recombinant
552 Booster Vaccine. *New England Journal of Medicine* **387**, 374-376,
553 doi:10.1056/nejmc2206711 (2022).
554 17 Sir Karakus, G. *et al. Preclinical efficacy and safety analysis of gamma-irradiated*
555 *inactivated SARS-CoV-2 vaccine candidates* (Cold Spring Harbor Laboratory,
556 2020).
557 18 Turan, R. D. *et al.* Gamma-irradiated SARS-CoV-2 vaccine candidate, OZG-
558 38.61.3, confers protection from SARS-CoV-2 challenge in human ACEII-
559 transgenic mice. *Scientific Reports* **11**, doi:10.1038/s41598-021-95086-4 (2021).
560 19 Khorattanakulchai, N. *et al.* Receptor binding domain proteins of SARS-CoV-2
561 variants produced in Nicotiana benthamiana elicit neutralizing antibodies
562 against variants of concern. *Journal of Medical Virology*, doi:10.1002/jmv.27881
563 (2022).
564 20 Winkler, E. S. *et al.* SARS-CoV-2 infection of human ACE2-transgenic mice causes
565 severe lung inflammation and impaired function. *Nature Immunology* **21**, 1327-
566 1335, doi:10.1038/s41590-020-0778-2 (2020).
567 21 Jiang, R.-D. *et al.* Pathogenesis of SARS-CoV-2 in Transgenic Mice Expressing
568 Human Angiotensin-Converting Enzyme 2. *Cell* **182**, 50-58.e58,
569 doi:10.1016/j.cell.2020.05.027 (2020).
570 22 Harvey, W. T. *et al.* SARS-CoV-2 variants, spike mutations and immune escape.
571 *Nat Rev Microbiol* **19**, 409-424, doi:10.1038/s41579-021-00573-0 (2021).

572 23 Tao, K. *et al.* The biological and clinical significance of emerging SARS-CoV-2
573 variants. *Nat Rev Genet* **22**, 757-773, doi:10.1038/s41576-021-00408-x (2021).
574 24 Zhao, X. *et al.* Neutralisation of ZF2001-elicited antisera to SARS-CoV-2 variants.
575 *Lancet Microbe* **2**, e494, doi:10.1016/S2666-5247(21)00217-2 (2021).
576 25 Brinkkemper, M. *et al.* A third SARS-CoV-2 spike vaccination improves
577 neutralization of variants-of-concern. *NPJ Vaccines* **6**, 146, doi:10.1038/s41541-
578 021-00411-7 (2021).
579 26 Branche, A. R. *et al. SARS-CoV-2 Variant Vaccine Boosters Trial: Preliminary*
580 *Analyses* (Cold Spring Harbor Laboratory, 2022).
581 27 Wang, Z. *et al.* A potent, broadly protective vaccine against SARS-CoV-2 variants
582 of concern. *NPJ Vaccines* **7**, 144, doi:10.1038/s41541-022-00571-0 (2022).
583 28 Chalkias, S. *et al.* Safety, immunogenicity and antibody persistence of a bivalent
584 Beta-containing booster vaccine against COVID-19: a phase 2/3 trial. *Nat Med*
585 **28**, 2388-2397, doi:10.1038/s41591-022-02031-7 (2022).
586 29 Dai, L. *et al.* Efficacy and Safety of the RBD-Dimer-Based Covid-19 Vaccine ZF2001
587 in Adults. *N Engl J Med* **386**, 2097-2111, doi:10.1056/NEJMoa2202261 (2022).
588 30 Xu, K. *et al.* Protective prototype-Beta and Delta-Omicron chimeric RBD-dimer
589 vaccines against SARS-CoV-2. *Cell* **185**, 2265-2278 e2214,
590 doi:10.1016/j.cell.2022.04.029 (2022).
591 31 Grigoryan, L. *et al.* Adjuvanting a subunit SARS-CoV-2 vaccine with clinically
592 relevant adjuvants induces durable protection in mice. *NPJ Vaccines* **7**, 55,
593 doi:10.1038/s41541-022-00472-2 (2022).
594 32 Gilbert, P. B. *et al.* A Covid-19 Milestone Attained - A Correlate of Protection for
595 Vaccines. *N Engl J Med*, doi:10.1056/NEJMp2211314 (2022).

596 33 Moss, P. The T cell immune response against SARS-CoV-2. *Nature Immunology*
597 **23**, 186-193, doi:10.1038/s41590-021-01122-w (2022).
598 34 Guerrera, G. *et al.* BNT162b2 vaccination induces durable SARS-CoV-2-specific T
599 cells with a stem cell memory phenotype. *Sci Immunol* **6**, eabl5344,
600 doi:10.1126/sciimmunol.abl5344 (2021).
601 35 Swanson, P. A., 2nd *et al.* AZD1222/ChAdOx1 nCoV-19 vaccination induces a
602 polyfunctional spike protein-specific T(H)1 response with a diverse TCR
603 repertoire. *Sci Transl Med* **13**, eabj7211, doi:10.1126/scitranslmed.abj7211
604 (2021).
605 36 Jara, A. *et al.* Effectiveness of homologous and heterologous booster doses for
606 an inactivated SARS-CoV-2 vaccine: a large-scale prospective cohort study.
607 *Lancet Glob Health* **10**, e798-e806, doi:10.1016/S2214-109X(22)00112-7 (2022).
608 37 Rouco, S. O. *et al.* Heterologous booster response after inactivated virus BBIBP-
609 CorV vaccination in older people. *Lancet Infect Dis* **22**, 1118-1119,
610 doi:10.1016/S1473-3099(22)00427-3 (2022).
611 38 Coria, L. M. *et al.* A Novel Bacterial Protease Inhibitor Adjuvant in RBD-Based
612 COVID-19 Vaccine Formulations Containing Alum Increases Neutralizing
613 Antibodies, Specific Germinal Center B Cells and Confers Protection Against
614 SARS-CoV-2 Infection in Mice. *Front Immunol* **13**, 844837,
615 doi:10.3389/fimmu.2022.844837 (2022).
616
617
618

Figure 1

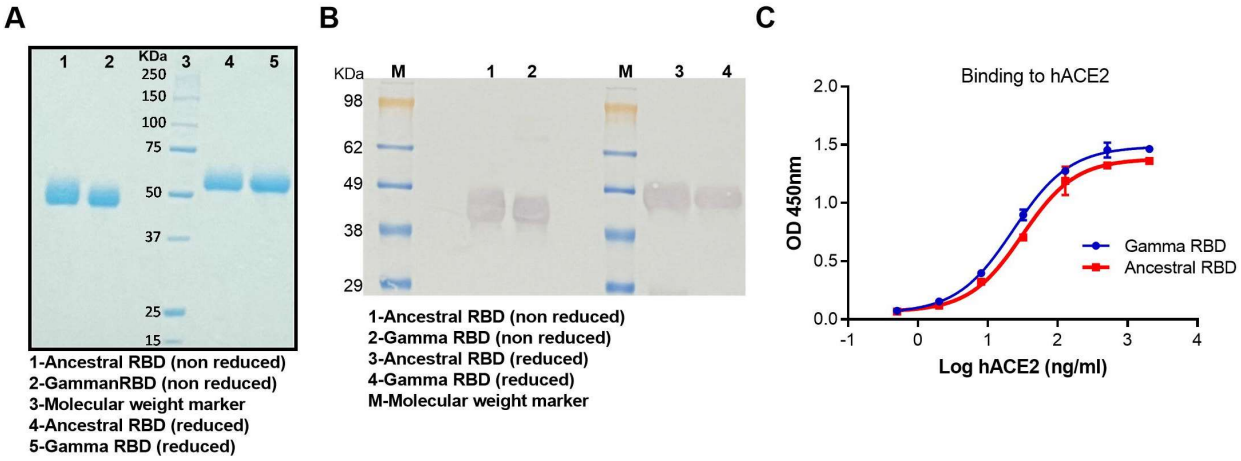

Figure 1. Characterization of RBD antigens. A. Non-reduced (nr) and reduced (r) SDS-PAGE migration profiles of the pooled samples (Gamma and ancestral RBD) are shown. **B**. **Western blot.** Non-reduced and reduced RBD antigens were detected using a rabbit polyclonal anti-RBD antibody. **C**. Binding affinity of Gamma and ancestral RBD proteins to immobilized human ACE2 receptor by ligand-receptor binding ELISA. Experiments were performed in duplicates and mean ± SD values are shown.

Figure 2

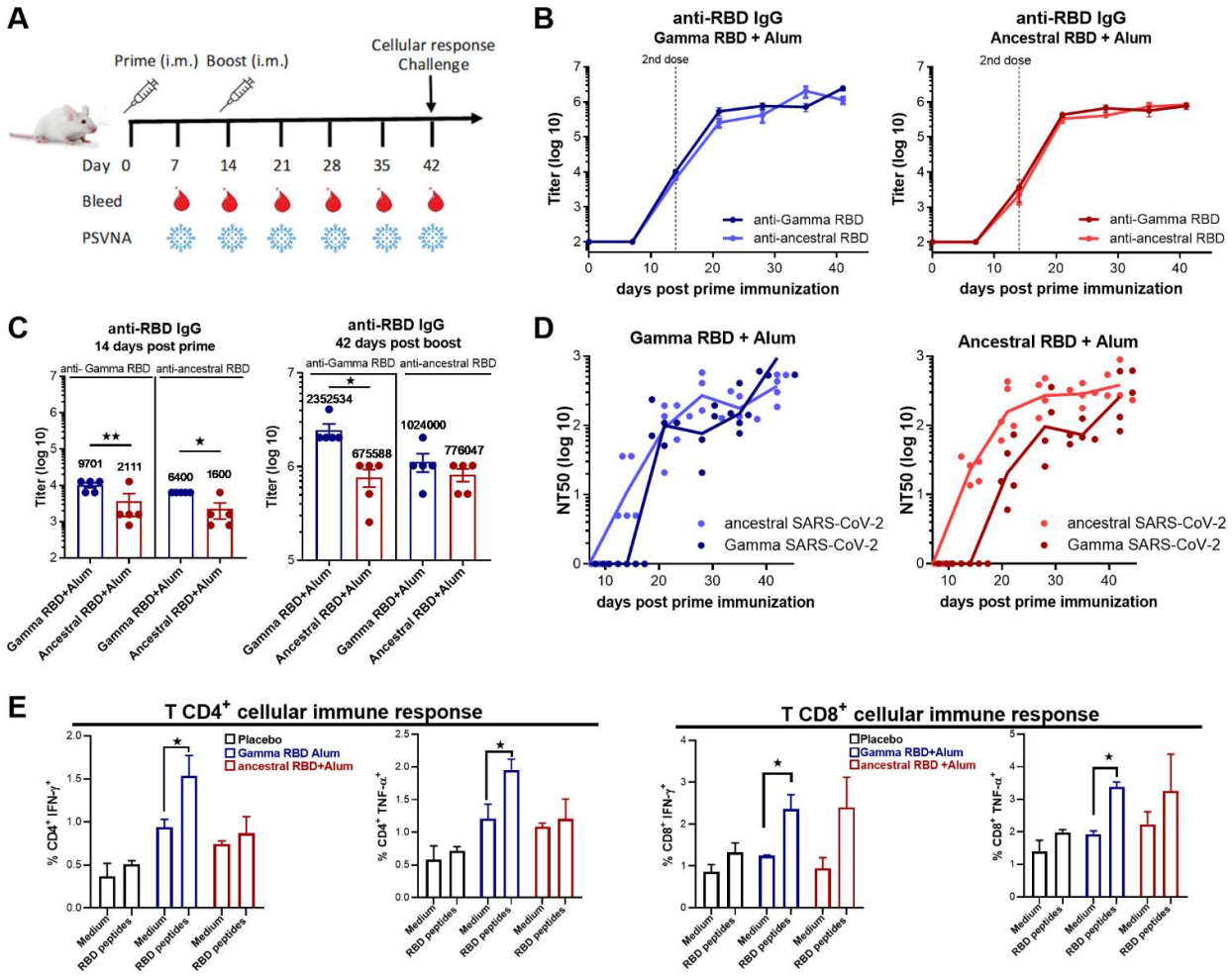

Figure 2. **Gamma RBD-adapted vaccine induce antibodies with a broad neutralizing activity and Ag-specific T cell responses**. **A**. Immunization protocol scheme. BALB/c mice were immunized at day 0 and day 14 via i.m. with: ancestral RBD + Alum (n=5), Gamma RBD + Alum (n=5). Serum samples were obtained at indicated time points for ELISA and neutralization assays. **B**. Kinetics of RBD-specific IgG endpoint titers in sera of immunized animals by ELISA. Points are means ± SEM. **C**. RBD-specific IgG titers in sera of immunized animals at day 14 and 42 post prime immunization. *p<0.05. **p<0.01. Mann Whitney test. **D**. Neutralizing-antibody titers in sera was determined by authentic PRNT SARS-CoV-2 assay for each group of vaccinated mice at different time points. The black lines represent the geometric mean (GMT) of all data points. Titers correspond to the 50% of virus neutralization (NT50). **E**. Mice were sacrificed 42 days after the first immunization to obtain spleens and lungs and T cell response was evaluated by intracellular flow cytometry. Splenocytes were stimulated with complete medium or RBD-peptides pool for 18 h and then brefeldin A was added for 5 h. Afterward, cells were harvested and stained with specific Abs anti-CD8, and anti-CD4, fixed, permeabilized, and stained intracellularly with anti–IFN-γ and anti-TNF-α. Results are presented as percentage of IFN-γ or TNF-α – producing T lymphocytes. Bars are means ± SEM. *p < 0.05 vs. medium. T test.

Figure 3

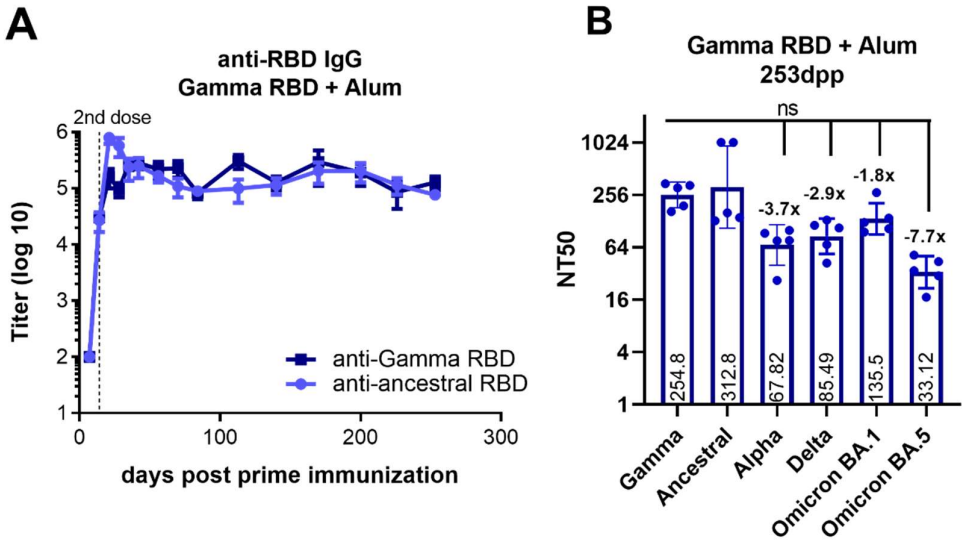

Figure 3. **Gamma RBD plus alum vaccinated mice induce a long-lasting antibody response with broaden neutralization activity**. BALB/c mice were immunized at day 0 and day 14 via i.m. with: Gamma RBD + Alum (n=5). **A**. Kinetics of RBD-specific (ancestral or Gamma) IgG endpoint titers in sera of immunized animals by ELISA until 253 days post prime immunization (dpp). Points are means ± SEM. **B.** Neutralizing-antibody titers against ancestral SARS-CoV-2 and different VOC (Alpha (B.1.1.7), Gamma (P.1) Delta (B.1.617.2) and Omicron (BA.1 and BA.5) were evaluated 253dpp in Gamma RBD +Alum immunized group. Neutralization titer was defined as the serum dilution that reduces 50% the cytopathic effect (NT50).

Figure 4

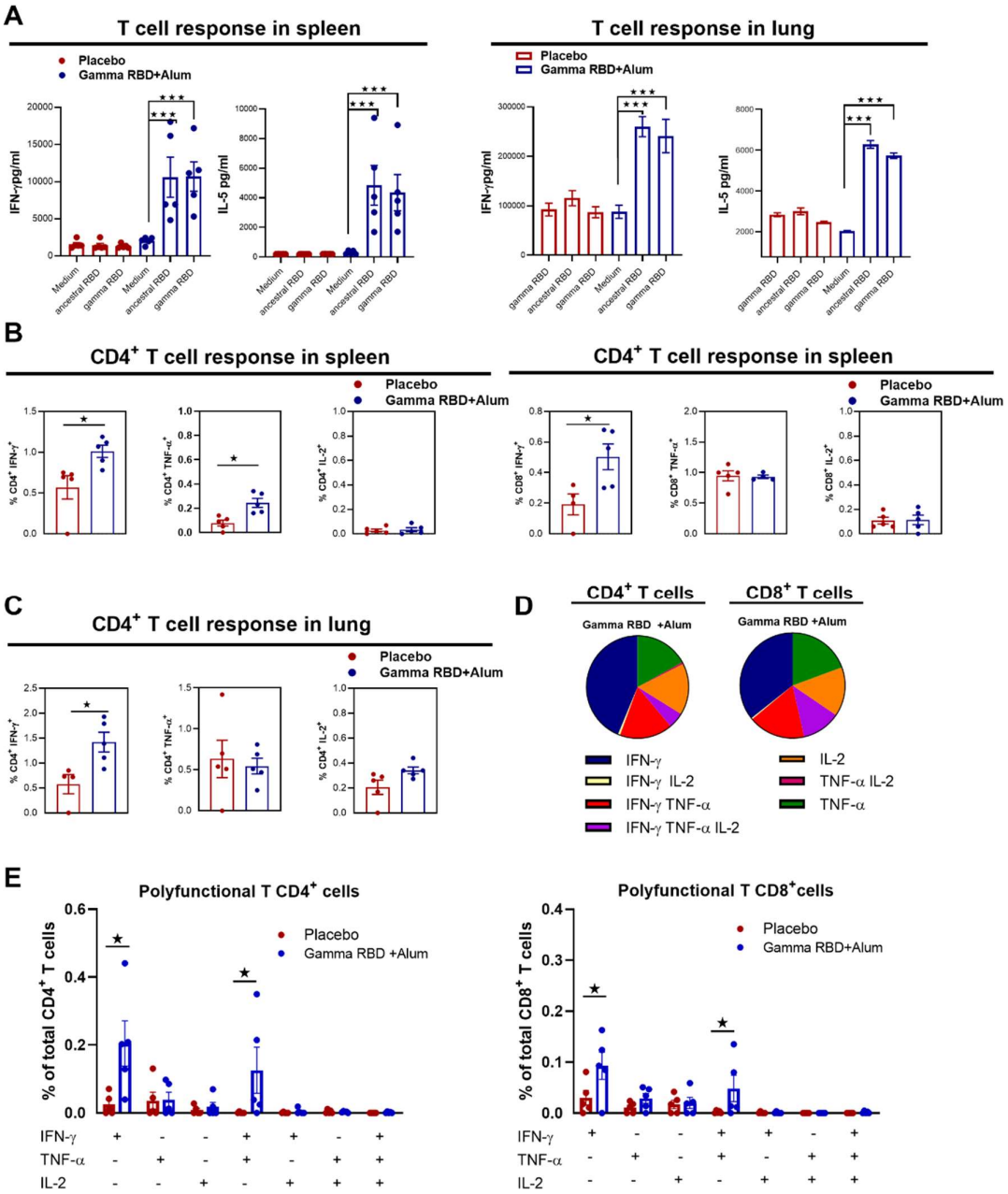

Figure 4. Gamma RBD formulated with alum induces T cell responses in mice. Cellular response was evaluated in spleen and lung 28 days after last immunization. **A**. Frequency of secreted IFN-γ and IL-5 following splenocytes or lung cells stimulation with medium or recombinant RBD were determined by ELISA. Bars are means ± SEM of pg/ml of IFN-γ and IL-5 after subtracting the amount in medium stimulated cells. *$p < 0.05$, **$p < 0.01$. T test. **Intracellular flow cytometry analysis of cytokine secreting T cells**. Splenocytes (**B**) and lung cells (**C**) were stimulated with complete medium or a peptide pool derived from RBD and then brefeldin A was added. Afterward, cells were harvested and stained with specific Abs anti-CD8, and anti-CD4, fixed, permeabilized, and stained intracellularly with anti–IFN-γ, TNF-α and anti-IL-2. Results are presented as percentage of cytokine-producing T cells. Bars are means ± SEM. *$p < 0.05$ vs. medium. T test. **D**. **Assessment of polyfunctional T cells**. Frequency of $CD4^+$ and $CD8^+$ T cells population from splenocytes that produce one, two or three cytokines were plotted for each group of mice. **E**. Pie graphs indicate the total proportion of RBD specific cytokine production in splenocytes from the Gamma RBD + Alum immunized mice.

Figure 5

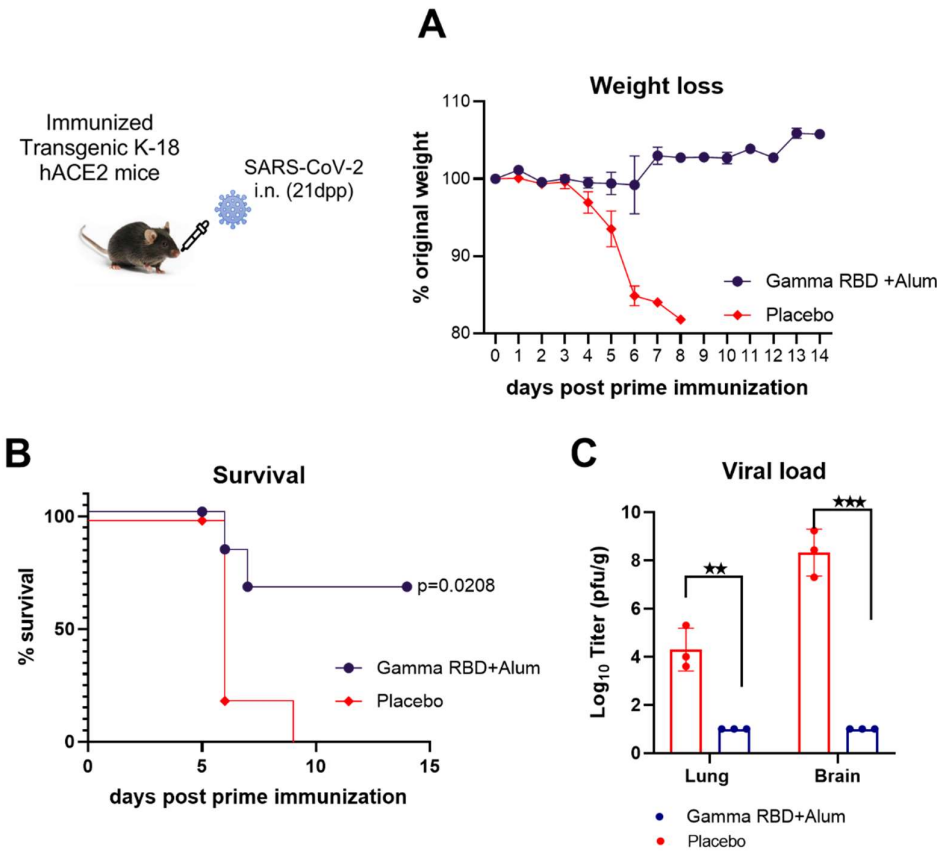

Figure 5. **Vaccination with Gamma RBD + Alum protects K18-hACE2 transgenic mice against intranasal SARS-CoV-2 infection**. Mice received PBS (Control) (n=8) or Gamma RBD + Alum (n=9) administered via i.m. route at day 0 and 14. Four weeks following immunization, K18-hACE2 mice were intranasally infected with 2×10^5 PFU of SARS-CoV-2. **A**. Weight changes in mice were monitored daily until day 14 after infection. Points are means ± SEM of percentage of original weight. **B**. Mice survival were monitored daily until day 14. Each dot represents the percentage of mice alive at that time point. Survival curves were analyzed with Log-rank (Mantel-Cox) test. P=0.0208 vs placebo. **C**. Five days after infection lungs and brains (n=3) were obtained from groups of mice and SARS-CoV-2 virus was titrated. Bars represent the mean ± SEM. $^{**}p < 0.01$ and $^{***}p < 0.001$. T test.

Figure 6

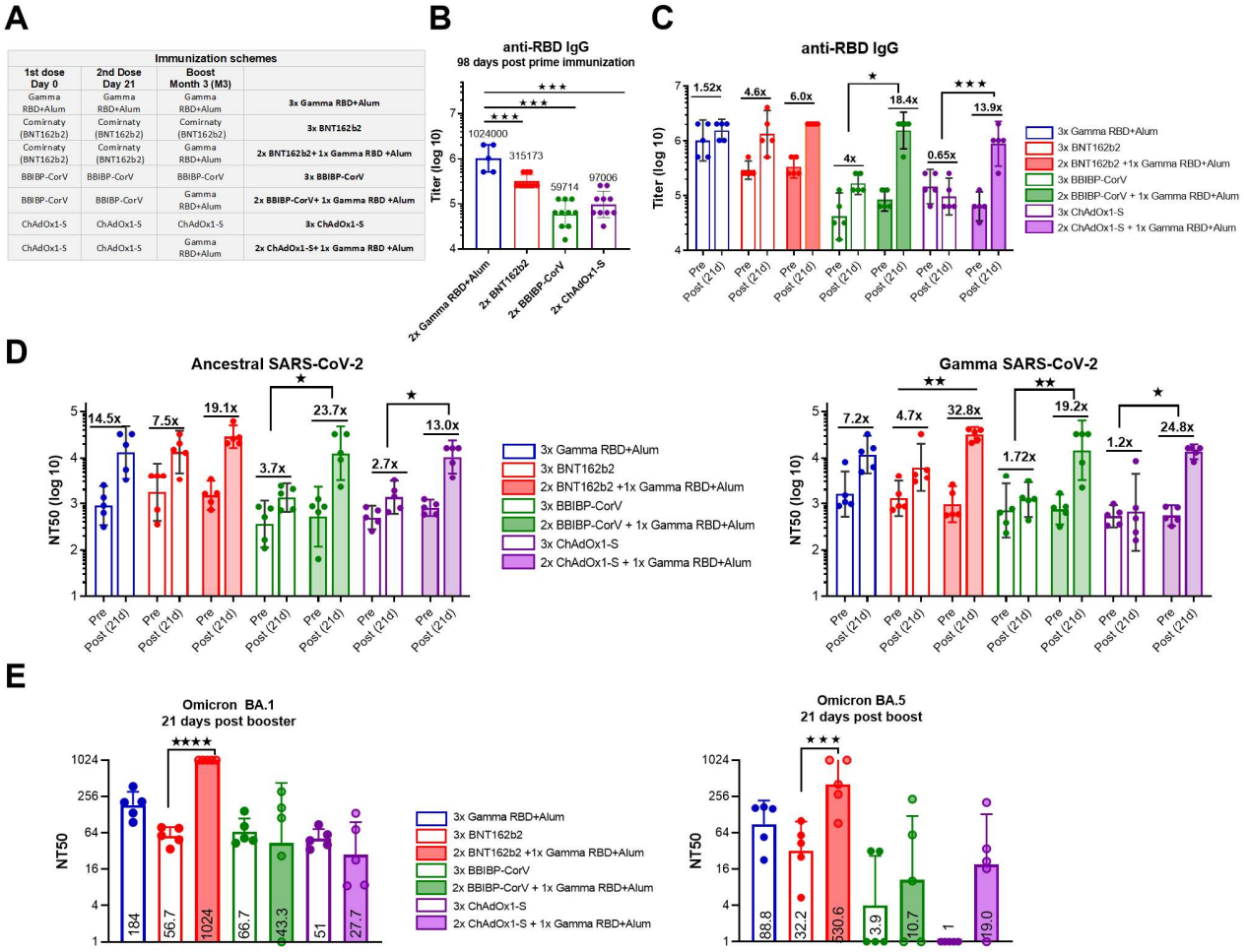

Figure 6. Heterologous boosting with Gamma RBD-adapted vaccine formulation of different primary vaccine platforms. **A**. Immunization protocol scheme. BALB/c mice were immunized at day 0 and day 21 via i.m. with: Gamma RBD + Alum (n=5), ChAdOx1-S (n=10), BNT162b2 (n=10) and BBIBP-CorV (n=10). At day 100 (M3) half of mice received homologous third doses (BNT162b2, BBIBP-CorV or ChAdOx1-S accordingly to table in A) and the other half heterologous booster shots with Gamma RBD + Alum. **B**. RBD-specific IgG titers in sera of immunized animals at day 98 post prime immunization. Bars are GMT ± 95% CI. *p<0.05. **p<0.01. Kruskal Wallis. Bars are GMT ± 95% CI. Numbers in bold are fold-increase in GMT values. **C**. Comparison of RBD-specific IgG titers pre and post-boost immunization. Numbers in bold are GMT fold-increase values. Bars are GMT ± 95% CI *p<0.05. ***p<0.001. Kruskal Wallis. **D**. Neutralizing-antibody titers against ancestral and Gamma SARS-CoV-2 were evaluated pre (98dpp) and post boost immunization (121 dpp) of mice. Neutralization titer was defined as the serum dilution that reduces 50% the cytopathic effect (NT50). Bars are GMT ± SD. Numbers in bold are fold-increase GMT values for each group. *p<0.05. ***p<0.001. Kruskal Wallis test. **E**. Neutralizing activity of antibodies against omicron (BA.1 and BA.5) were evaluated 21 days post boost immunization of mice. Neutralization titer was defined as the serum dilution that reduces 50% the cytopathic effect (NT50). Bars are GMT ± SD and numbers are GMT values for each group of mice. *p<0.05. ***p<0.001. Kruskal Wallis test.